PRAMANA — journal of physics
© Indian Academy of Sciences
Vol. 74, No. 1
January 2010
pp. 67–74

The double-end-pumped cubic Nd:YVO_4 laser: Temperature distribution and thermal stress

P ELAHI[1,*] and S MORSHEDI[2]
[1]Department of Physics, College of Science, Shiraz University of Technology, Shiraz, Iran
[2]Department of Physics, Payame Noor University, Shiraz, Iran
*Corresponding author. E-mail: elahi@sutech.ac.ir

MS received 21 January 2009; revised 26 May 2009; accepted 30 July 2009

Abstract. Thermal effects of a double-end-pumped cubic Nd:YVO_4 laser crystal are investigated in this paper. A detailed analysis of temperature distribution and thermal stress in cubic crystal with circular shape pumping is discussed. It has been shown that by considering the total input powers as constant, the double-end-pumped configurations with equal pump power can be considered as having a minimum thermal effect with respect to the other end-pumped configuration.

Keywords. Cubic crystals; double-end-pumping; thermal effects.

PACS Nos 42.55.f; 42.55.Xi

1. Introduction

Diode-end-pumped solid-state lasers are of great interest due to their high efficiency, compact package and high beam quality. They are outstanding due to their wide industrial and medical applications. The thermal effects such as thermal lensing and stress, influence the performance of these lasers especially in high power regime which have been studied in [1,2]. These thermal effects, originating from the induced heat and temperature gradient, influence the optical behaviour of the laser crystal and can even move the resonator stability position in the plane of the stability curve. To design these laser resonators, the thermal effects cannot be neglected. Many methods have been proposed for reducing thermal effects. The use of composite crystals [3,4], designing the variable configuration resonators [5] and double-end-pumping scheme are some of them [6]. The rectangular crystals have great potential for reducing the thermal effects because of their great coolant surface [7–10]. In this paper, we consider the cubic Nd:YVO_4 laser crystal which possesses broad absorption peak, large stimulated emission cross-section, linearly polarized output, etc.

The temperature distribution and the thermal effects such as thermal stress have been investigated for double-end-pumped laser crystal. We discussed the

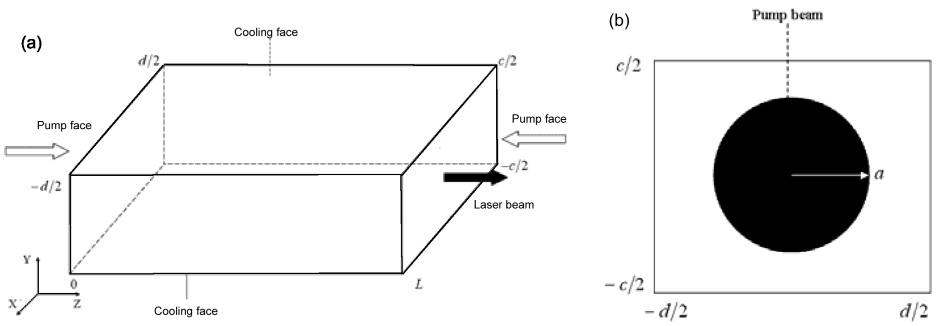

Figure 1. Schematic diagram of the double-end-pumped cubic crystal: (**a**) The pump beam of the crystal is along the z-direction and heat is removed from four sides of the surfaces. (**b**) Pump dimension on the x–y plane.

temperature in the crystal in various pump and found the optimum thermal-safe configuration.

2. Temperature distribution

The geometry of the double-end-pumped cubic crystal is shown in figure 1. The crystal dimensions are $d \times c \times L$ which are pumped from two end faces ($z = 0, z = L$) by two diode lasers. The optical axis of the crystal is along z-direction and the direction of the output laser beam is in the same direction as the pump beam.

The steady-state heat conduction equation for an anisotropic medium on the Cartesian coordinate system is [11]

$$K_x \frac{\partial^2 T}{\partial x^2} + K_y \frac{\partial^2 T}{\partial y^2} + K_z \frac{\partial^2 T}{\partial z^2} = -Q(x, y, z), \tag{1}$$

where K_x, K_y and K_z are the thermal conductivities along x, y, and z directions, $Q(x, y, z)$ is the heat generation per unit volume and T is the temperature.

The pump beam can be assumed to have an inhomogeneous intensity with a Gaussian profile along the x, y-direction. By considering the propagation along the z-axis, the heat power density can be written as

$$\begin{aligned} Q(y, z) = \Bigg[& Q_{\mathrm{l}} \exp\left(\frac{-(x^2 + y^2)}{\omega_{\mathrm{l}}^2(z)} \right) \exp(-\alpha z) \\ & + Q_{\mathrm{r}} \exp\left(\frac{-(x^2 + y^2)}{\omega_{\mathrm{r}}^2(z)} \right) \exp(-\alpha(L - z)) \Bigg], \end{aligned} \tag{2}$$

where α is the absorption coefficient of the crystal in input power and n is the refractive index of the crystal. Q_{l} (Q_{r}) are the left (right) heat power density and can be calculated as

$$Q_{\mathrm{l}} = \frac{\eta P_{\mathrm{l}}}{2\pi \int_0^a \int_0^L \exp(-r^2/\omega_{\mathrm{l}}^2(z)) \exp(-\alpha z) r \,\mathrm{d}r \,\mathrm{d}z}, \tag{3a}$$

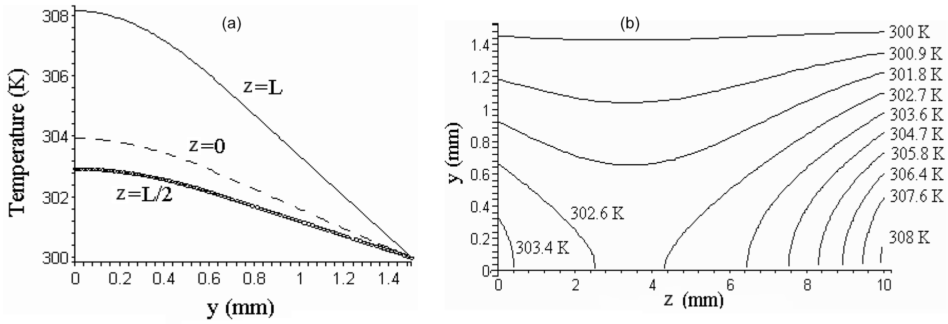

Figure 2. Temperature distributions in double-end-pumped cubic crystal. The left and right input power is 3 W and 7 W respectively. (**a**) Temperature along y-direction at $z = 0, L/2, L$. (**b**) Contour graph.

$$Q_{\rm r} = \frac{\eta P_{\rm r}}{2\pi \int_0^a \int_0^L \exp(-r^2/\omega_{\rm l}^2(z)) \exp(-\alpha(L-z)z) r \,{\rm d}r \,{\rm d}z} \tag{3b}$$

In the above equations, $P_{\rm l}$ ($P_{\rm r}$) is the left (right) input power. The heat generating coefficient due to quantum defect $\eta = 1 - \lambda_{\rm Pump}/\lambda_{\rm laser}$ and $\omega_{\rm l}(z)$ and $\omega_{\rm r}(z)$ are the left and right pump spot sizes respectively and can be written as

$$\omega_{\rm l}(z) = \omega_0 \sqrt{1 + \left[\frac{M^2 \lambda_{\rm P} z}{n\pi\omega_0^2}\right]^2}, \tag{4a}$$

and

$$\omega_{\rm r}(z) = \omega_0 \sqrt{1 + \left[\frac{M^2 \lambda_{\rm P} (L-z)}{n\pi\omega_0^2}\right]^2}. \tag{4b}$$

The wavelength of diode lasers and output beam are 808 nm and 1064 nm respectively. We consider the c-cut Nd:YVO$_4$ cubic crystal with 0.5% doping concentration and 2.7 cm^{-1} absorption coefficient at 808 nm. The dimensions of the crystal are $d = c = 3$ mm and $L = 10$ mm. The propagation of the shaped pump beam can be approximately described as a Gaussian beam and consider $M = \sqrt{10}$. The minimum beam waist is about $\omega_0 = 0.75$ mm. The thermal conductivities along the axis are $K_x = K_y = 5.1$ W/mK and $K_z = 5.23$ W/mK. Using the following boundary conditions including the continuity of temperature and gradient on the boundary of the pump region means

$$T_{\rm pump}(r = a) = T_{\rm unpump}(r = a), \tag{5}$$

and

$$\frac{\partial T_{\rm pump}(r = a)}{\partial T} = \frac{\partial T_{\rm unpump}(r = a)}{\partial T}. \tag{6}$$

Newtonian boundary condition of cooling is

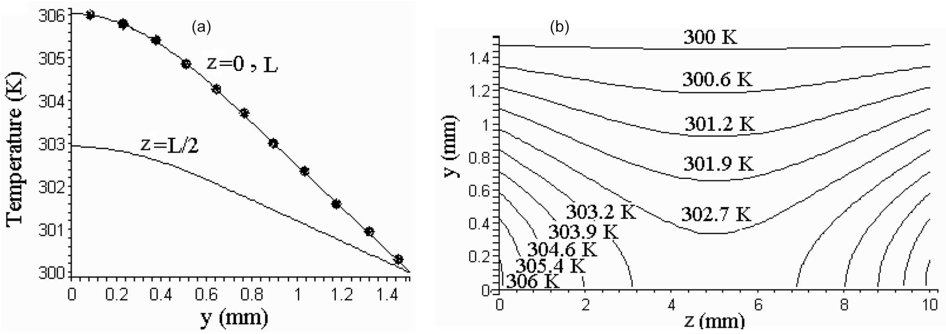

Figure 3. Temperature distributions in double-end-pumped crystal. The left and right input power is 5 W. (**a**) Temperature along y-direction at $z = 0, L/2, L$. (**b**) Contour graph.

$$\left.\frac{\partial T_{\text{unpump}}(r)}{\partial x}\right|_{x=d/2 \text{ and } -d/2} = \frac{h}{K_x}[T_{\text{c}} - T_{\text{unpump}}(r)|_{x=d/2 \text{ and } -d/2}], \quad (7)$$

and

$$\left.\frac{\partial T_{\text{unpump}}(r)}{\partial y}\right|_{y=c/2 \text{ and } -c/2} = \frac{h}{K_y}[T_{\text{c}} - T_{\text{unpump}}(r)|_{y=c/2 \text{ and} -c/2}], \quad (8)$$

where T_{c} is the coolant temperature ($T_{\text{c}} = 300$ K) and h is the convective coefficient. Figure 2 shows the 2D and the contour plots of temperature distribution in the crystal with $P_{\text{l}} = 3$ W and $P_{\text{r}} = 7$ W on the y-axis ($x = 0$).

As seen from these figures, the maximum temperature is about 308 K which is the temperature on the right of the crystal. The temperature on the left rises to 303.4 K approximately in this case. Figure 3 shows the temperature distribution in double-end-pumped configuration with equal input power of 5 W on both the left and right sides.

The maximum temperature rise is 306 K in this pumping configuration which is smaller than the maximum temperature in double-end-pump with different pumping. For comparison, graphs of temperature distribution with single pump configuration with total pump power of 10 W are shown in figure 4.

As can be seen from this figure, the maximum temperature is about 310.9 K which is about 1.6% greater than in equal double pumping. Although this temperature difference is negligible in this regime, it will be noticeable in high power pumping which is shown in figure 5.

As can seen in the case of double equal pumping with $P_{\text{l}} = P_{\text{r}} = 100$ W, the maximum temperature rises to 418 K approximately, which is about 24.4% smaller than single pumping with the same total power. So in high power regime, the double equal pumping is more thermal safe with respect to the other pump configuration and in this case the thermal-induced effects such as thermal aberration will be decreased. It is important to note that thermal aberrations like thermal spherical aberrations influence the beam quality and poor beam quality occurs when we neglect them. In figure 6, the maximum temperature in the crystal vs. minimum

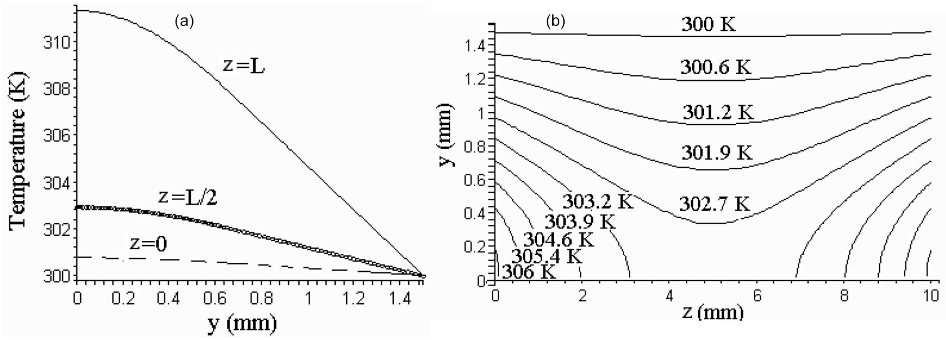

Figure 4. Temperature distributions in single-end-pumped crystal: (**a**) Temperature along y-direction at $z = 0, L/2, L$. (**b**) Contour graph.

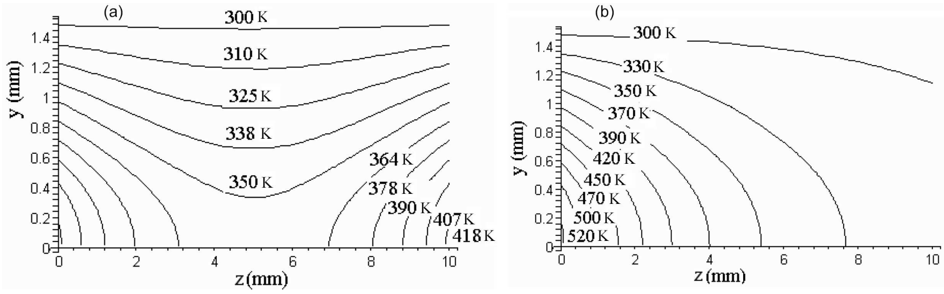

Figure 5. Contour plot of temperature distribution in (**a**) double equal pumping with $P_{\rm l} = P_{\rm r} = 100$ W and (**b**) single pumping with $P = 200$ W.

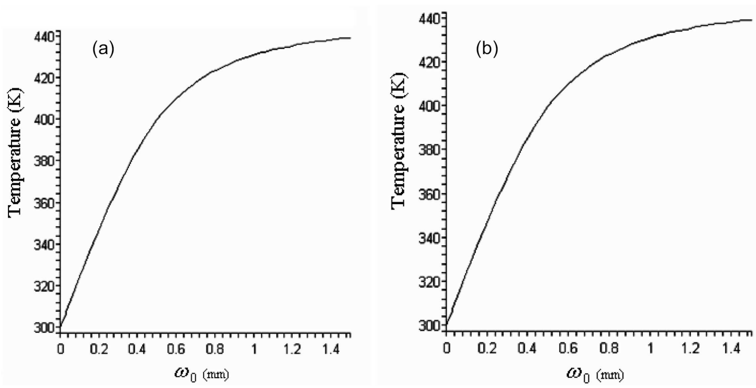

Figure 6. Maximum temperature in the crystal vs. ω_0. (**a**) In equal double pumping with $P_{\rm l} = P_{\rm r} = 5$ W, (**b**) $P_{\rm l} = P_{\rm r} = 100$ W.

spot size of the pump source are plotted in equal double pumped configuration with 5 W and 100 W. A fast variation of temperature in small values of minimum spot size is noticeable.

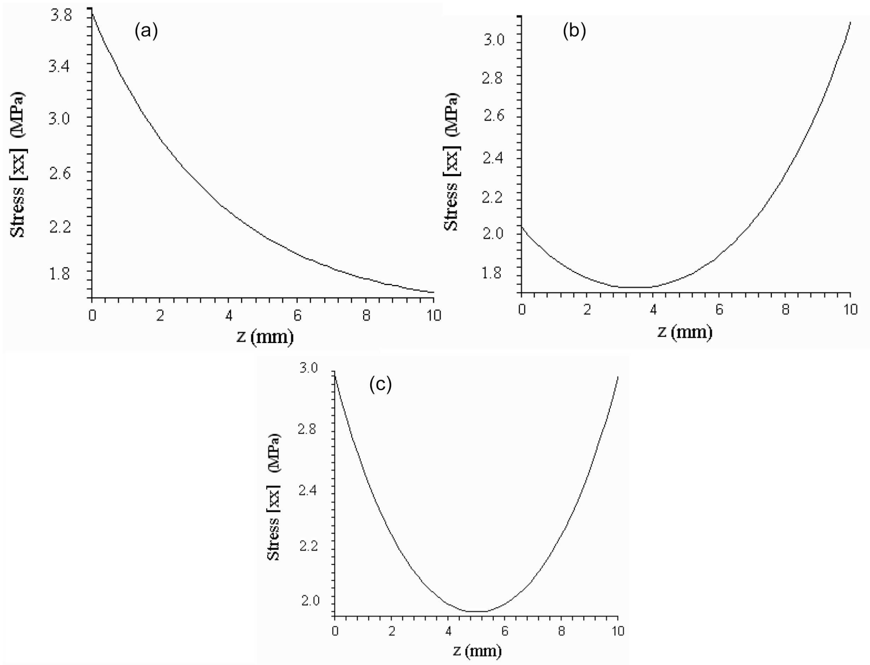

Figure 7. σ_{xx} component of stress vs. z in $y = 0$. (**a**) Single pump with $P_{\mathrm{l}} = 10$ W, (**b**) double pump with $P_{\mathrm{l}} = 3$ W and $P_{\mathrm{r}} = 7$ W and (**c**) double pump with $P_{\mathrm{l}} = P_{\mathrm{r}} = 5$ W.

3. Thermal stress

In the absence of the thermal loading, the crystal is assumed to be stress-free and not constrained by external forces. The thermal-induced stress distributions are generated by the temperature gradients and can be calculated as [12]

$$\sigma_r = \frac{\alpha_a E}{1-\nu}\left[\frac{1}{a^2}\int_0^a \Delta T(r,z) r\,\mathrm{d}r - \frac{1}{r^2}\int_0^r \Delta T(r,z) r\,\mathrm{d}r\right], \tag{9}$$

$$\sigma_{zz} = \frac{\alpha_c E}{1-\nu}\left[\frac{2\nu}{b^2}\int_0^a \Delta T(r,z) r\,\mathrm{d}r - \Delta T(r,z)\right], \tag{10}$$

where E is the Young's modulus ($E = 1.33 \times 10^{11}$), ν is the Poisson ratio ($\nu = 0.33$), α is the thermal expansion coefficient ($\alpha_c = 11.37 \times 10^{-6}$/K and $\alpha_a = 4.43 \times 10^{-6}$/K). The xx component of the thermal stress, that means σ_{xx}, for three various pump configurations vs. z in $y = 0$ are plotted in figure 7. As can be seen from these figures, in single-end-pumping the maximum stress rises to 3.8 MPa while in double with equal pumping it rises to 2.9 MPa approximately. The maximum and minimum stress difference in single with $P_{\mathrm{l}} = 10$ W, double with

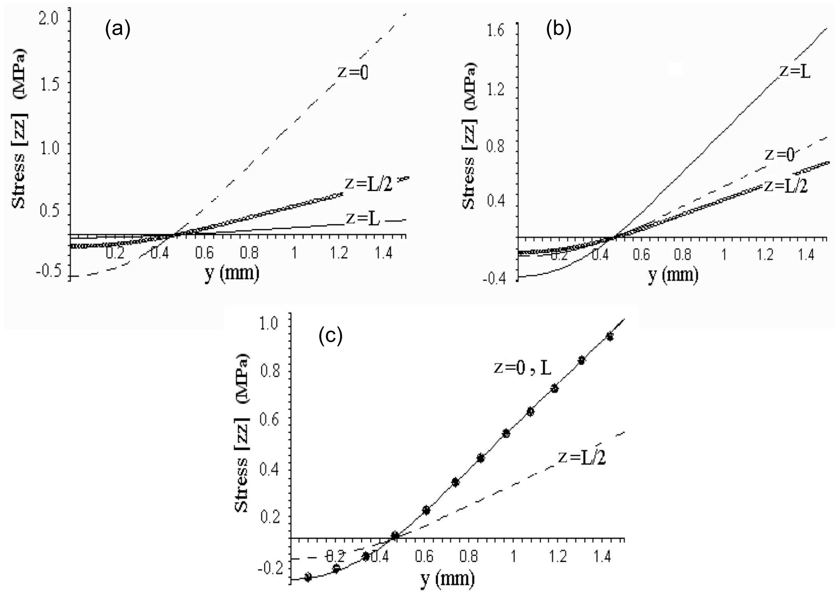

Figure 8. σ_{zz} component of stress vs. y in $x = 0$. (**a**) Single pump with $P_\mathrm{l} = 10$ W, (**b**) double pump with $P_\mathrm{l} = 3$ W and $P_\mathrm{r} = 7$ W and (**c**) double pump with $P_\mathrm{l} = P_\mathrm{r} = 5$ W.

$P_\mathrm{l} = 3$ W and $P_\mathrm{r} = 7$ W and double with $P_\mathrm{l} = P_\mathrm{r} = 5$ W is 2 MPa, 1.3 MPa and 0.9 MPa respectively. The same plot for σ_{zz} is plotted in figure 8. The minimum stress and minimum stress difference are shown in equal double pumping.

4. Conclusion

In the present work, the temperature distribution and thermal stress of the actual double-end-pumped Nd:YVO$_4$ cubic crystal have been discussed. The results show that by considering the input power as a constant, the double configuration with equal pumping has minimum temperature effect and stress. So it is more thermal safe with respect to the other configurations and we do not have to worry about the unexpected damage.

References

[1] Fuyan Lu, Mali Gong, Haizong Xue, Qiang Liu and Wupeng Gong, *Opt. Laser Eng.* **45**, 43 (2007)
[2] H Nadgaran and P Elahi, *Pramana – J. Phys.* **66(3)**, (2006)
[3] M P MacDonald, Th Graf, J E Balmer and H P Weber, *Opt. Commun.* **78**, 383 (2000)
[4] Th Graf, E Wyss, M Roth and H P Weber, *Opt. Commun.* **190**, 327 (2001)
[5] Ai-Yun Yao *et al*, *Chin. Phys. Lett.* **22(3)**, 607 (2005)

[6] Hamish Ogilvy, Michael J Withford, Peter Dekker and James A Piper, *Opt. Express* **11(19)**, 2411 (2003)
[7] J Eggleston, T J Kane, K Kuhn, J Unternahrer and R L Byer, *IEEE J. Quantum Electron.* **20**, 289 (1984)
[8] T J Kane, J M Eggleston and R L Byer, *IEEE J. Quantum Electron.* **21**, 1195 (1985)
[9] Zhe Ma, Daijun Li, Jiancum Gao, Nianle We and Keming Du, *Opt. Commun.* **275**, 179 (2007)
[10] M Sabaeian, H Nadgaran and L Mousave, *Appl. Optics* **47(13)**, 2317 (2008)
[11] W Koechner, *Solid-state laser engineering* (Springer Verlag, Berlin, 2006) 6th edn
[12] S P Timoshenko and J N Goodier, *Theory of elasticity* (McGraw-Hill, San Francisco, CA, 1970)